Microbial population dynamics are dominated by stochastic forces in a low biomass subseafloor habitat

Rika E. Anderson*[a‡], Elaina D. Graham[b], Julie A. Huber[c], Benjamin J. Tully*[b,d‡]

a. Biology Department, Carleton College. Northfield, MN
b. Department of Biological Sciences, University of Southern California, Los Angeles, CA
c. Marine Chemistry and Geochemistry, Woods Hole Oceanographic Institution, Woods Hole, MA
d. Center for Dark Energy Biosphere Investigations, University of Southern California, Los Angeles, CA

* To whom correspondence should be directed
Dr. Rika Anderson
Biology Department, Carleton College. Northfield, MN
E-mail: randerson@carleton.edu

Dr. Benjamin Tully
Department of Biological Sciences
Center for Dark Energy Biosphere Investigations
University of Southern California, Los Angeles, CA
E-mail: tully.bj@gmail.com

‡ These authors contributed equally to this work

Abstract

The subseafloor is a vast global habitat that supports microorganisms that have a global scale impact on geochemical cycles. Much of the subseafloor contains endemic microbial populations that consist of small populations under growth-limited conditions. For small population sizes, the impacts of stochastic evolutionary events can have large impacts on intraspecific population dynamics and allele frequencies. These conditions are fundamentally different than those experienced by most microorganisms in surface environments, and it is unknown how small population sizes and growth-limiting conditions influence evolution and population structure. Using a two-year, high-resolution environmental time-series, we examine the dynamics of 10 microbial populations from cold, oxic crustal fluids collected from the subseafloor site North Pond, located near the mid-Atlantic ridge. The 10 microbial populations were divided into groups with distinct patterns of population dynamics based on abundance, nucleotide diversity, and changes in allele frequency. Results reveal rapid allele frequency shifts linked to different types of population interactions, including sweeps, dispersal, and clonal expansion. Dispersal plays an important role in structuring the most abundant populations in the crustal fluids. Microbial populations in the subseafloor of North Pond are highly dynamic and evolution is governed largely by the stochastic forces of dispersal and drift.

Importance

The cold, oxic subseafloor is an understudied habitat that is difficult to access, yet important to global biogeochemical cycles and starkly different compared microbial habitats on the surface of the Earth. Our understanding of microbial evolution and population dynamics has been largely molded by studies of microbes living in surface habitats that can host 10-1,000 times more microbial biomass than has been observed in the subsurface. This study provides an opportunity to observe evolution in action within a low biomass, growth-limited environment and reveals that while microbial populations in the subseafloor can be influenced by changes in selection pressure and small-scale gene sweeps, the stochastic forces of genetic drift and dispersal have an important impact on the evolution of microbial populations. Much of the microbial life on the planet exists under growth-limited conditions and the subseafloor provides a natural laboratory to explore these fundamental biological questions.

Introduction

The marine subsurface is home to more than half of the archaea and bacteria inhabiting the oceans[1,2]. Marine subsurface habitats are frequently energy-limited environments, which impacts the total biomass that can be supported in these environments[3]. As a result, microbial communities in these habitats are composed of relatively small populations[4-6] (<10^4 cells per unit volume). Population size can have important consequences for how microbial populations evolve over time, and factors such as genetic drift can have an exaggerated impact on small microbial populations compared to habitats in which microbial populations are larger. Most previous studies of adaptation in natural microbial communities have focused on habitats with high biomass and thus larger population sizes, such as the surface ocean, deep-sea hydrothermal vents and freshwater lakes[7-10]. It is unclear how natural selection and genetic drift shape the evolution of microbial communities in low-biomass habitats, despite the fact that a substantial fraction of global microbial biomass is found in such habitats.

North Pond, located near the mid-Atlantic ridge, offers a unique opportunity to examine dynamics of microbial adaptation in natural populations in a low-biomass, growth-limited habitat[11]. The North Pond site consists of exposed crustal ridges with a depression that has accumulated <100 m of low permeability sediment, resulting in the bulk of fluid exchange and transport to occur beneath the sediment basin. This subseafloor aquifer connects the deep waters of the oceans through a porous network of crustal rock, which globally contains about 2% of the oceans' volume[12-14]. The crustal aquifer beneath the sediments of North Pond is accessible through two circulation obviation retrofit kits (CORKs) installed in 2011, providing direct access to the fluids circulating within the aquifer, while preventing exchange with the overlaying water and sediment environments[15,16]. Repeated sampling in 2012, 2014, and 2017, including an eight sample *in situ* time-series collected from 2012-2014, has revealed a dynamic microbial community with a high degree of functional redundancy in a complex hydrological system depleted in dissolved organic carbon (DOC)[6,17-19]. The aquifer microbial communities are distinct from bottom seawater, and there are multiple lines of genetic evidence to suggest that the microbial community within the aquifer is motile and metabolically flexible, with the ability to carry out both autotrophic and organotrophic pathways [6,17,20]. The North Pond subseafloor microbial community is low biomass[6,20] (10^3-10^4 cells ml^{-1}) and incubation experiments suggest the North Pond microbial community is growth-limited and that increasing temperature and enrichment with DOC result in rapid growth (E. Trembath-Reichert, S. R. Shah Walter, M. A. Fontánez, P. D. Carter, P. R. Girguis, J. A. Huber, submitted for publication).

It has been hypothesized that in energy- and growth-limited environments, such as low-deposition deep-sea sediments, adaptive mutations would be unable to sweep through populations and mutations would accumulate as a result of energy limitation[21]. However, the crustal aquifer does not reflect the limited fluid flow and isolated cellular environments in low-energy sediments. North Pond fluids are

86 capable of traversing distances of approximately[19] 2-40 m day^{-1}, though this fluid flux is spatially and
87 temporally complex, resulting in convective and oscillatory fluid movement rather than linear flow along
88 the North-South axis[22]. Fluid movement appears to impact the microbial community, as previous analysis
89 of the system revealed discrete ecological units within the time-series that would oscillate between
90 presence and absence with extended time periods (*e.g.*, 100s of days) between reoccurrences[6]. However,
91 it is unclear how this dynamic environment impacts natural selection and genetic drift on the endemic
92 microbial populations.
93 Here, we present an analysis of the intraspecific population dynamics of the North Pond aquifer
94 microbial community from a time series spanning 10 time points over a two-year period. We show that
95 abundant microorganisms within the aquifer have patterns of genome diversity where large-scale genomic
96 sweeps are infrequent and small gene sweeps, genetic drift, and dispersal of populations from the larger
97 metapopulation within the aquifer may have a more pronounced impact on genome diversity. The
98 metagenomic samples collected from North Pond between 2012-2014 present a unique opportunity to
99 explore microbial population dynamics on short timescales and provide new understanding as to how
100 microorganisms adapt and persist in the largest habitat on the planet.
101
102 **Materials and methods**
103 *Sample collection and sequencing*
104 As has been described elsewhere[6,19,20], North Pond water samples were collected from two CORKs at
105 holes U1382A and U1383C in 2012 and 2014. For sample time points (TP) during expeditions (TP0 in
106 April 2012 and TP9 in April 2014), the Mobile Pumping System (MPS) attached to the *ROV* Jason II was
107 used to collect samples through umbilical lines connecting the CORK platform to fluids in the aquifer.
108 For samples collected between expeditions (TP1-TP8), the battery powered GEOMicrobeSled[23,24]
109 deployed on the CORK collected samples approximately every two months. In all instances, lines were
110 purged to remove stagnant water prior to sampling and all samples were fixed with RNALater *in situ*. A
111 complete set (n = 8) of *in situ* samples were collected from U1382A and provide the necessary samples
112 and resolution for downstream analysis (as described below). Previously described in Tully *et al.*[6], DNA
113 was extracted from filters using a phenol chloroform method[25] and paired-end sequencing was performed
114 on an Illumina HiSeq 1000 at the Marine Biological Laboratory. Raw sequences were quality controlled
115 using Cutadapt[26] v1.7.1 (parameters: -e 0.08 - -discard-trimmed - -overlap = 3) and Trimmomatic[27] v0.33
116 (parameters: PE SLIDINGWINDOW:10:28 MINLEN:75).
117
118 *Metagenome-assembled genomes and manual curation*

To build upon the set of MAGs generated in Tully *et al.*[6], the quality controlled paired end reads were assembled using three different approaches to maximize recovery of MAGs that had previously remained unbinned. A detailed methodology has been provided in the Supplementary Information and a comprehensive assessment of the final set of MAGs can be found in Supplemental Data 1.

SNV identification and analysis

anvi'o[28] v5.0 contig databases were generated for all MAGs. FASTA files of the contigs of each MAG were converted to an anvi'o database (anvi-gen-contigs-database --skip-mindful-splitting). Bowtie2[29] v2.3.4.1 (parameters: --no-unal) was used to create recruitment profiles for each MAG in each sample. The output SAM format file was converted to a sorted BAM format file using samtools[30] v1.9 and reads with <95% sequence identity over 75% of the alignment were filtered from the recruitment profile using BamM v1.7.3 (parameters: --percentage_id 0.95 --percentage_aln 0.75; https://github.com/Ecogenomics/BamM). Recruitment profiles were merged with anvi-merge. During the anvi-profile step, the flag --profile-SCVs was set to include identification of single nucleotide variants (SNVs) and single codon variants (SCVs). Each individual MAG anvi'o database had the collection value 'DEFAULT' and bin value 'EVERYTHING' added using anvi-script-add-default-collection. Using those collection and bin values, anvi-gen-variability-profile with default parameters and the flags --engine AA, --include-contig-names, and --engine CDN to extract SNV, single amino acid variants (SAAVs), and SCVs, from the profiles of each MAG in each North Pond sample (Supplemental Data 2). The SCV and SAAV values were used to calculate pN/pS ratios using anvi-script-calculate-pn-ps-ratio (anvi'o v6.2).

The sorted, filtered BAM format recruitment profiles described above were used to determine read counts for each contig using featureCounts[31] v1.5.3 (default parameters) as implemented within Binsanity-profile[32] v0.3.3 (default parameters). Read counts were converted to the normalized unit reads per kilobase pair MAG per Megabase pair of metagenomic sample (RPKM; Supplemental Data 3). Read counts were also used to determine the relative fraction of each MAG in each metagenomic sample and combined with cell count data collected as part of Tully *et al.*[6] (Eq. 1) to estimate the number of cells per MAG present in each sample (Supplemental Data 4).

$$Eq.\,1\ (reads\ recruited\ to\ MAG/total\ reads\ in\ metagenomic\ sample)\ x\ cells\ per\ mL$$

It is important to note that without sufficient controls, all metagenomic data is compositional in nature and is impacted by numerous biases of sampling and sequencing methodology[33]. Thus, estimates of cell abundances derived from metagenomic data should be considered to be imprecise estimates of absolute abundance[21].

U1382A provided a high-resolution sample dataset (10 time points over ~825 days) and MAGs detected in these samples were selected for downstream analysis based on two criteria from the time

series: (1) sufficient coverage (≥5 RPKM) in ≥3 time points or (2) high coverage (≥30 RPKM) in at least 1 time point. Only time points that had ≥5 RPKM were considered for SNV calculations. This criterion was set to ensure that most base pairs in each MAG had at least 20× read coverage, which would be required to reliably call SNVs. As has been reported previously[34-36], MAGs tend to represent a cohesive population represented by a >95% nucleotide identity boundary. To confirm that a majority of the signal for each population came from closely related organisms, RPKM values were recalculated and compared using recruited reads filtered to 99% identity over 75% of the length of the alignment using BamM (parameters: --percentage_id 0.99 --percentage_aln 0.75; Supplemental Data 3). Two of the MAGs (NORP143 and NORP246) were taxonomically assigned to the genus *Shewanella* and shared 98.2% ANI, as determined with FastANI[35]. For consideration of this analysis these MAGs were deemed to represent the same species-level population and NORP143 (67.24% complete, 9.87% redundancy) was removed from downstream analysis while NORP246 was retained (82.57% complete, 2.28% redundancy; Table 1). The features identified in NORP246 were confirmed by creating a new anvi'o database with recruited reads filtered to 99% identity over 75% of the length of the alignment (as above). To ensure consistency of presentation, all analysis below was based on anvi'o databases constructed using recruited reads filtered to 95% identity over at least 75% of the length of the alignment.

Table 1. Genome statistics, taxonomic assignment, relative abundance values for persister and bloomers designated MAGs.

						Calendar Date	25-Apr-12	6-Aug-12	5-Oct-12	4-Dec-12	2-Feb-13	3-Apr-13	2-Jun-13	1-Aug-13	30-Oct-13	5-Apr-14
						Julian Days	116	219	279	339	399	459	519	579	669	826
Classification	MAG ID	Complete (%)	Redundancy (%)	Strain Heterogeneity (%)	Length (bp)	GTDB Taxonomy	TP0 (RPKM)	TP1 (RPKM)	TP2 (RPKM)	TP3 (RPKM)	TP4 (RPKM)	TP5 (RPKM)	TP6 (RPKM)	TP7 (RPKM)	TP8 (RPKM)	TP9 (RPKM)
Persister	NORP83	68.26	0.87	100.00	2,484,891	(o) Rhizobiales	0.02	16.62	0.23	13.69	11.27	2.73	9.95	1.04	0.38	0.00
	NORP139	65.80	0.39	100.00	1,500,119	(f) Parvibaculaceae	2.13	6.84	6.90	4.37	9.78	8.50	6.97	1.27	1.21	0.01
	NORP147	64.94	2.41	14.29	2,818,071	(f) Rhizobiaceae	0.00	36.41	0.08	20.33	12.36	0.11	0.30	0.02	0.02	0.03
	NORP163	85.59	0.35	14.29	2,163,954	(c) Gammaproteobacteria	20.86	16.51	48.66	3.43	2.92	1.12	0.24	19.77	20.95	2.97
	NORP169	97.79	0.74	33.33	2,915,406	(g) Nitratireductor_B	2.12	6.53	5.09	0.82	0.52	1.43	8.38	4.84	4.14	0.08
	NORP246	82.57	2.28	52.94	4,176,188	(g) Shewanella	0.02	11.60	0.10	8.34	5.24	1.74	0.12	0.10	0.13	0.00
Bloomer	NORP6	82.65	0.60	0.00	3,242,937	(g) Desulforhopalus	0.00	0.00	0.00	0.00	88.61	0.00	0.02	0.00	0.00	0.00
	NORP57	98.28	4.42	78.26	5,236,658	(g) Halomonas	0.04	0.00	0.00	0.00	0.00	0.00	0.00	0.00	0.00	38.25
	NORP100	94.63	2.69	0.00	4,801,899	(o) Thiohalomonadales	1.05	0.10	1.97	0.08	0.16	0.11	0.01	2.46	2.77	38.98
	NORP167	58.25	0.00	0.00	2,959,101	(f) Flavobacteriaceae	0.03	30.13	0.07	0.13	0.01	0.00	0.00	0.01	0.00	0.00

Functional annotation and taxonomic assignment

Protein sequences as determined within anvi'o were submitted to the GhostKOALA KEGG annotation and mapping service[37] (Submitted 23 October 2018; parameters: genus_prokaryotes + family_eukaryotes). KEGG annotations were added to the anvi'o contig databases for each MAG using the Python script KEGG-to-anvio (https://github.com/edgraham/GhostKoalaParser) and anvi-import-functions (http://merenlab.org/2018/01/17/importing-ghostkoala-annotations/).

GTDB-Tk[38] v1.3.0 (classify_wf default parameters) using database R95 was used to determine a taxonomic assignment for each MAG.

Data transformations for analysis

181 The SNV occurrence table generated by anvi'o was filtered by retaining all entries with >0 entropy value,
182 SNV positions ≥20× coverage in the time point(s) of interest, and if the departure from consensus was
183 ≥0.10. Putative SNVs at each time point were converted to nucleotide diversity (SNVs kbp^{-1})[21] based on
184 the full length of the MAG (Supplemental Data 2). Time points for which a MAG was present at <5
185 RPKM were not used to calculate SNVs kbp^{-1} or considered in further analysis.
186 Majority allele frequency was calculated by identifying the consensus allele for each position and
187 dividing the number of occurrences of that allele by the total coverage for that site. For each MAG, mean
188 majority allele frequency was determined by averaging all majority allele frequencies for each SNV
189 across the entire MAG. Positions for which no SNV was recorded were assumed to be fixed at the
190 reference allele in the contig. If the consensus allele did not match the reference allele in the contig, then
191 the position was assumed to be fixed at the consensus allele. Hierarchical clustering was performed and
192 plotted using seaborn (doi: 10.5281/zenodo.3767070) with the default clustermap settings (average
193 distance linkage method and Euclidean distance metric).
194 For each MAG, gene coverage values were exported from the anvi'o databases using anvi-export-
195 gene-coverage-and-detection. Gene frequency in a sample was calculated by dividing each gene coverage
196 value by the median coverage value of all genes. Genes of interest were identified based on changes in
197 gene frequency such that the maximum frequency value minus the minimum frequency value in the time
198 points of interest was ≥1. Genes identified in this manner lacking a KEGG annotation were compared
199 against GenBank nr using BLASTP (Supplemental Data 5). Hierarchical clustering was performed and
200 plotted using seaborn, as above.
201 Putative genes were assigned to the broad KEGG categories (*e.g.*, carbohydrate metabolism,
202 energy metabolism, *etc*.) based on KEGG annotations (Supplemental Data 6). For each MAG, the
203 calculated pN/pS ratios for all putative genes within each KEGG category was compared in a pairwise
204 manner against the relevant time points (≥5 RPKM) with the Mann-Whitney U test[39] and Benjamini-
205 Hochberg[40] corrected *p*-values assuming a 5% false discovery rate. pN/pS values for KEGG categories
206 with significant difference between time points were plotted as box and swarm plots with seaborn.
207
208 **Results and Discussion**
209 *Improving North Pond metagenome-assembled genomes*
210 By comparing and combining the total set of new MAGs to the original 2018 NORP MAGs[6] (n = 997
211 MAGs), it was possible to replace 22 2018 NORP MAGs with newly reconstructed MAGs with higher
212 completion and/or lower redundancy statistics and to produce 137 completely new MAGs, previously
213 unrecovered from the metagenomic datasets (Supplemental Data 1). Additional results and discussion of
214 these MAG results can be found in the Supplementary Information.

Intraspecific population diversity of microbes in North Pond fluids

To conduct a robust analysis of genome dynamics at borehole U1382A over the two-year time series, we focused on MAGs that occurred in at least three samples with ≥5 RPKM (Table 1; Figure 1; Supplemental Data 3). In total, six MAGs met these criteria. The set of mapped metagenomic reads to each MAG represents the overall population diversity of a corresponding microbial population. Therefore, the terms "MAG" and "population" are used interchangeably for the remainder of the manuscript. To reflect the fact that the populations represented by these MAGs persisted in multiple samples, the group was defined as "persisters." We identified another four MAGs with high coverage (>30 RPKM) in only one sample. In all four instances, these MAGs had low coverage (<3 RPKM) in the other time points, with three having extremely low coverage at other time points (<0.15 RPKM) (Table 1; Figure 1; Supplemental Data 3). This group of four MAGs were defined as "bloomers." As reviewed in Van Rossum *et al.*[41], variation with populations is added and removed through soft sweeps, genetic drift, and dispersal. Through this lens, we conducted an in-depth analysis of these 10 MAGs to better understand the impacts of dispersal, genome sweeps, and drift on microbial populations in the aquifer. Due to the complexity of fluid movement within the aquifer, it is challenging to distinguish between dispersal and drift, thus we assumed that rapid shifts in population structure were likely associated with dispersal, but in all instances, drift may contribute to or cause the observed shifts.

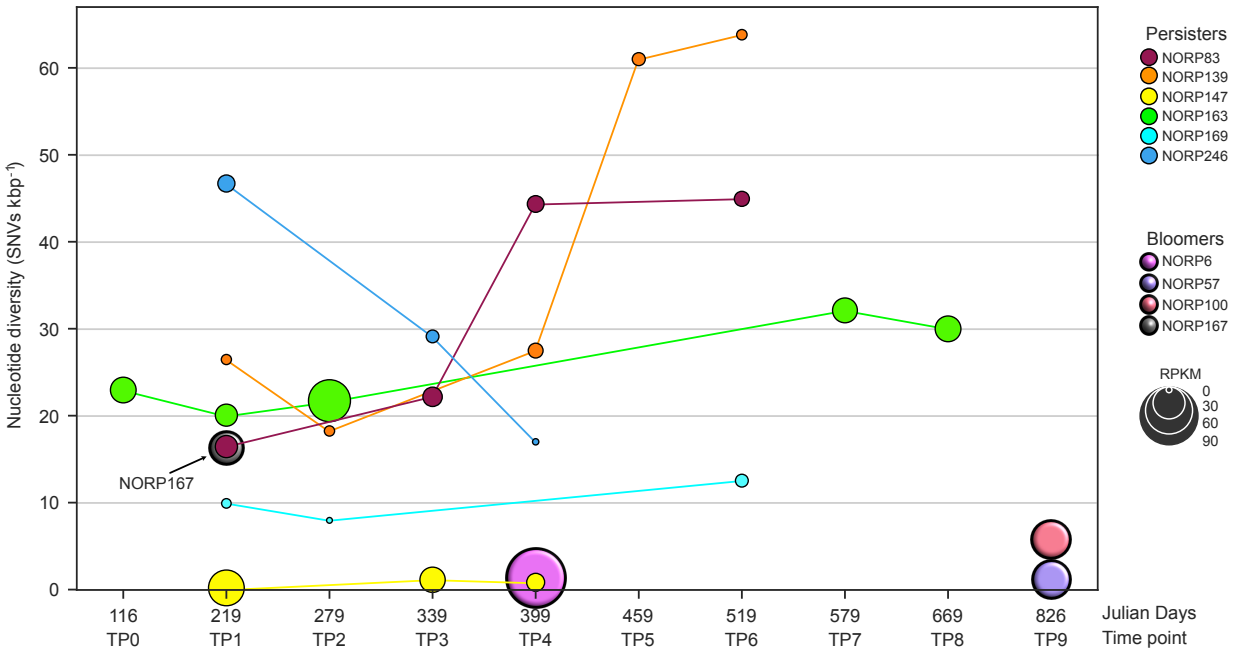

Figure 1. Scatter plot of the nucleotide diversity for each of the six "persister" and four "bloomer" MAGs for the ten time points sampled from North Pond CORK U1382A. The size of each point is scaled by the RPKM in the time point. Only time points with ≥ 5 RPKM are included. Lines denote points from the same MAG and do not display continuous data.

233 *Low nucleotide diversity and clonal expansion.* We designated MAGs demonstrating a sudden abundance
234 increase as "bloomers," suggesting they had undergone rapid growth in the subseafloor (Table 1). Thus,
235 these MAGs were candidates for a putative clonal expansion. Clonal expansions occur when a population
236 undergoes rapid growth, usually due to expansion into a new niche, and subsequently does not have
237 enough time to accumulate mutations within the population[42]. We used single nucleotide variants (SNVs)
238 per kilobase pair as a measure of genomic diversity within the populations represented by these MAGs.
239 NORP6 and NORP57 had low nucleotide diversity (<2 SNVs kbp^{-1}) and low abundance (<0.04 RPKM;
240 equivalent to approximately <1 cell mL^{-1}) in all other time points except for the "bloom" time point of
241 interest (Figure 1, Table 1). The low observed nucleotide diversity suggested that these particular
242 populations may have undergone a recent clonal expansion relative to the other populations (Figure 1).
243 The other two "bloomers," NORP100 and NORP167, do not show the reduced nucleotide
244 diversity expected for a clonal expansion and instead seem to have undergone rapid changes in abundance
245 due to the movement of populations through the borehole. NORP100 was found in high abundance (38.98
246 RPKM; equivalent to approximately 5,209 cells mL^{-1}) at a single time point (T9) but had a higher
247 nucleotide diversity (5.7 SNVs kbp^{-1}) compared to NORP6 and NORP57 (Figure 1). Unlike the other two
248 "bloomers," NORP100 was present in the preceding time points (TP7 and TP8) but at low abundance
249 (2.46 and 2.77 RPKM, respectively; equivalent to approximately 211 and 65 cells mL^{-1}, respectively),
250 suggesting that the higher observed nucleotide diversity for NORP100 may be the result of accumulation
251 of mutations in the nine months between TP7 and TP9, followed by a period of growth. As such, this
252 increase in abundance from TP8 to TP9 may represent growth of multiple co-occurring genotypes, and
253 not a single clonal expansion. In contrast, NORP167 appeared to be an example of dispersal rather than
254 clonal expansion. NORP167 was virtually absent from the preceding time point (TP0; 0.03 RPKM;
255 equivalent to approximately <1 cell mL^{-1}), but was observed at TP1 with relatively high nucleotide
256 diversity (16.3 SNVs kbp^{-1}), and subsequently a more complex population structure, unlike the expected
257 population structure after a clonal expansion. The high diversity observed in NORP167 suggested that the
258 observed population may have migrated into the borehole prior to (or during) sampling from elsewhere
259 within the aquifer.
260 For the four populations labeled as "bloomers," SNV analysis was limited to a single time point.
261 For the six populations labeled as "persisters," multiple time points were used to assess the role of
262 selection, drift, and dispersal on the population (Figure 1). The population represented by the MAG
263 NORP147 (unknown *Rhizobiaceae*) displayed genomic variation patterns indicative of clonal expansion
264 followed by dispersal through the aquifer (Figure 2A). NORP147 transitioned from no/low abundance to
265 high abundance twice during the sampling period (between TP0-TP1 and between TP2-TP3), which may
266 correspond to two separate clonal expansion events (Table 1). The NORP147 intraspecific TP1-

population had low nucleotide diversity (0.2 SNVs kbp^{-1}) and a corresponding allele frequency indicating that most alleles were fixed. The subsequent populations in TP3 and TP4 had a slightly elevated nucleotide diversity (1.12 and 0.84 SNVs kbp^{-1}, respectively), and new alleles were introduced and then removed from the population from TP1 to TP3 and TP3 to TP4, respectively (Figure 2B). For the NORP147 population, selection pressure did not appear to change over time, as the SAAV/SNV ratio remained constant and none of the KEGG categories had significant changes in pN/pS values (Supplemental Data 6). Therefore, while the low nucleotide density and dominance of specific alleles indicate that TP1-population resulted from a recent clonal expansion, the high diversity of allele variants in TP3 and TP4 suggest that patterns of nucleotide variation fluctuated in the NORP147 population between time points, most likely through dispersal of members of the metapopulation within the aquifer. Similar rapid accumulation of SNVs in the human gut have been linked to the introduction of a new strain as opposed to the accumulation of thousands of mutations[43]. Further, several small co-localized segments across the genome maintained an allele frequency of ~0.5 in all three time points, suggesting that several parts of the genome maintained genotypic diversity independent of the shifting population structure even in the TP1-population after experiencing a clonal expansion (Supplemental Figure 2A).

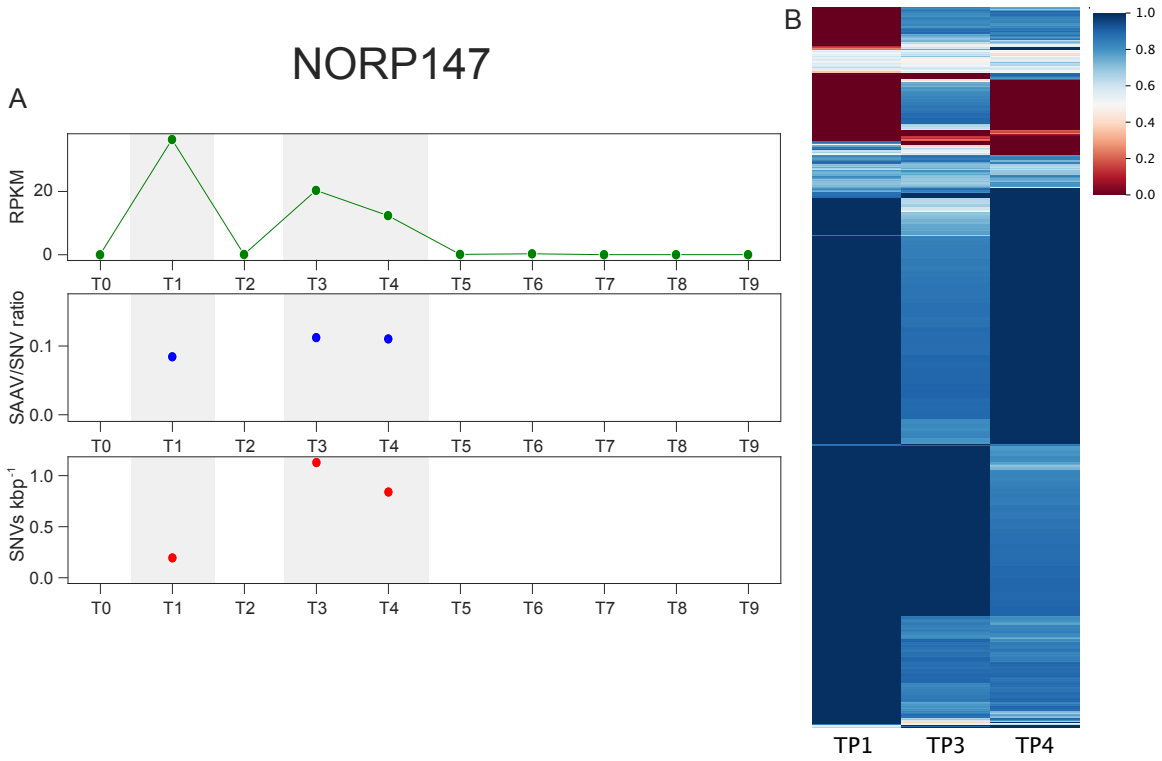

Figure 2. Intraspecific population metrics for NORP147. **A.** Scatterplots tracking RPKM, SAAV/SNV ratio, and SNVs kbp^{-1} across the time-series. Grey boxes highlight the time points of interest (≥ 5 RPKM). SAAV/SNV ratio and SNVs kbp^{-1} in low abundance time points have been removed. **B.** Hierarchically clustered heatmap of allele frequency at each identified SNV location. Scaled from 0-1. Both 0.0 and 1.0 represent a fixed allele; 0.5 represents a split allele.

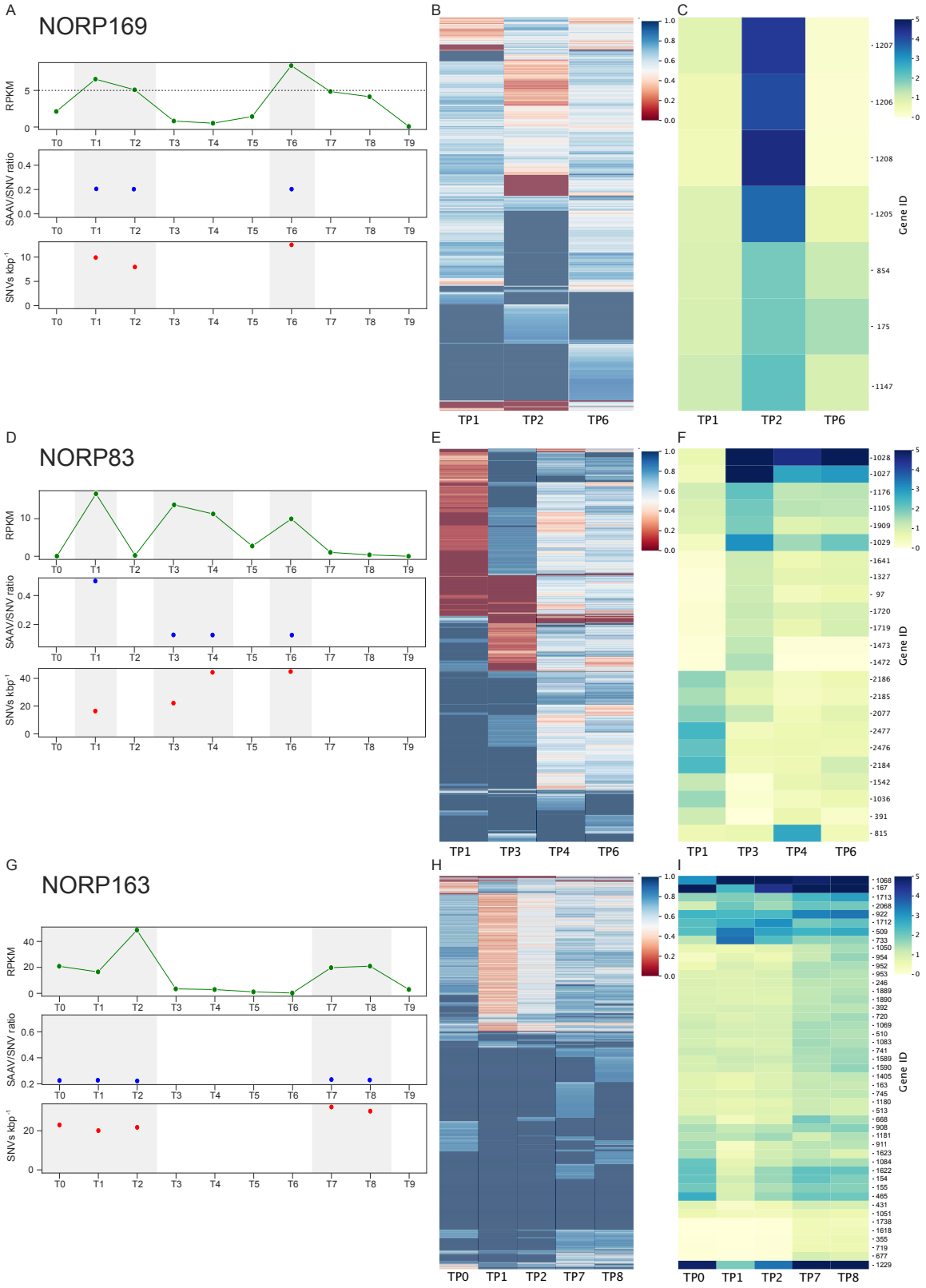
A
NORP169
RPKM
SAAV/SNV ratio
SNVs kbp⁻¹
T0 T1 T2 T3 T4 T5 T6 T7 T8 T9
B
TP1 TP2 TP6
C
Gene ID
TP1 TP2 TP6
D
NORP83
E
TP1 TP3 TP4 TP6
F
TP1 TP3 TP4 TP6
G
NORP163
H
TP0 TP1 TP2 TP7 TP8
I
TP0 TP1 TP2 TP7 TP8

283

Figure 3. Intraspecific population metrics for NORP83, NORP163, and NORP169. **A, D, G.** Scatterplots tracking RPKM, SAAV/SNV ratio, and SNVs kbp^{-1} across the time-series. Grey boxes highlight the time points of interest (≥5 RPKM). SAAV/SNV ratio and SNVs kbp^{-1} in low abundance time points have been removed. The y-axes across MAGs are not held constant. **B, E, H.** Hierarchically clustered heatmap of allele frequency and identified SNV location. Scaled from 0-1. Both 0.0 and 1.0 represent a fixed allele; 0.5 represents a split allele. **C, F, I.** Hierarchically clustered heatmap of gene frequencies for genes ≥1× change in coverage over the time points of interest. Scaled range from 0-5× copies. Maximum value of gene frequency in F and G is 9.5× and 6.5× copies, respectively. Supplemental Data 5.

Dispersal as a major driver of population structure. While the dynamics between clonal growth and dispersal may be difficult to assess in the "bloomers," and NORP147 showed evidence of both clonal growth and dispersal, dispersal through the aquifer appeared to have played a major role in influencing the population structure of four "persister" MAGs (NORP83, NORP163, NORP169, and NORP246). For these four "persisters," there was an extensive amount of underlying intraspecific diversity and most experienced large shifts between allele frequencies over relatively short timescales (Figures 3 and 4). The changes in allele frequencies were more dynamic and stochastic than has been observed previously in other habitats, such as the surface ocean, deep-sea hydrothermal vents and freshwater lakes[10,34,44], suggesting that the genomic diversity we observed was created by the movement of multiple populations through the crustal aquifer rather than consistent selection on a specific population over time.

Due to the observed high nucleotide diversity, both NORP169 (*Nitratireductor_B*) and NORP83 (unknown *Rhizobiales*) were identified as candidate populations that have been molded by dispersal (Figure 3A-F). NORP169 had sufficient coverage in three time points (TP1, TP2, TP6; Figure 3A) and NORP83 had sufficient coverage in four time points (TP1, TP3, TP4, TP6; Figure 3D) to accurately call SNVs. Both MAGs experienced drops in abundance (≤ 0.82 RPKM; equivalent to approximately ≤ 22 cells mL^{-1}) between time points, and it is unclear if these sharp changes resulted from migration or cell death. The observed nucleotide diversity in each MAG also changed across the time points of interest (Figure 3A & D). The observed nucleotide diversity remained relatively constant for NORP169 (8.0-12.5 SNVs kbp^{-1}) while that of NORP83 more than doubled over the time points of interest (16.4 to 44.9 SNVs kbp^{-1}).

Despite differences in how nucleotide diversity changed over time, the rapidly shifting patterns of allele frequency in both of these populations indicated the dispersal of at least two competing dominant genotypes within each population. Patterns of allele frequency for NORP169 revealed a complex dynamic between co-existing populations (Figure 3B). Specifically, while nucleotide diversity suggested that there was little difference between TP1 (9.9 SNVs kbp^{-1}) and TP2 (8.0 SNVs kbp^{-1}), the allele frequency reveals that TP2 represented an entirely different intraspecific population compared to TP1 and TP6 (Figure 3B). The rapid transition from the TP1-population to the TP2-population (60 days), followed by low abundance in intervening time points, and a return to allele frequencies similar to those of the TP1-population at TP6, suggests that either dispersal or drift, rather than selection, may have influenced genotypic diversity. Given the relatively rapid changes in allele frequency between TP1 and TP2 (Figure

314 3B), and without the corresponding decrease in nucleotide diversity indicative of clonal expansion or
315 population bottleneck, dispersal seems the likeliest explanation for the genome dynamics observed here.
316 Further, the data suggests that selection had a limited impact on genome diversity within this population,
317 as SAAV/SNV ratio remained constant (Figure 3A) and none of the putative genes assigned to KEGG
318 categories have changes in the observed pN/pS ratio (Supplemental Data 6). The populations at different
319 time points also possessed different sets of genes based on observed changes in gene frequency (≥1×
320 change in coverage between time points; Figure 3C): for example, the TP2-population possessed a co-
321 localized set of putative genes (NORP169 Gene IDs 1205-1208) that shifted from <1× copies per genome
322 in TP1 and TP6 to ~4× copies per genome in TP2 and an additional three genes that fluctuated between
323 1× and 2× copies per genome (Figure 3C). While none of these putative genes had KEGG annotations,
324 several of the functional assignments from GenBank implicated transcriptional regulation possibly related
325 to plasmid replication (Supplemental Data 5). It is possible the region encompassing gene IDs 1205-1208
326 represents an integrated extrachromosomal element within the NORP169 TP2-population.
327 Unlike NORP169, NORP83 showed substantial accumulation of mutations in the genome over
328 the four time points of interest (Figure 3E). But like NORP169, the patterns in allele frequency suggest
329 that the genotypic population was completely different from TP1 to TP3 with more than half of the sites
330 represented by a different dominant allele compared to TP1 (Figure 3E). Abundance of NORP83 dropped
331 in the intervening time point (0.23 RPKM; equivalent to approximately 5 cells mL^{-1}) implicating either
332 migration or cell death (Figure 3D). The underlying TP4-population reveals that many of the SNV sites
333 were split between two alleles (~0.5 allele frequency), suggesting a mixed population (Figure 3E). While
334 abundance dropped in TP5 below the threshold for accurately calling SNVs (2.73 RPKM), the allele
335 patterns in TP6 appeared similar to those in TP4. One possible explanation for these patterns is dispersal:
336 at least two populations of NORP83, captured separately in TP1 and TP3, mixed together in TP4 and TP6
337 and resulted in the doubling of the nucleotide diversity between TP3 and TP4. Alternatively, this
338 population structure may be the result of genetic drift: the decrease in abundance at TP2 may have
339 resulted in a small population that "reset" the allele frequencies, though the high nucleotide diversity
340 (22.17 SNVs kbp^{-1}) in TP3 make such a clonal expansion unlikely. While the SAAV/SNV ratio remained
341 low and constant over the four time points of interest, there was a statistically significant shift in pN/pS
342 ratio for the broad "No KEGG annotation" category for putative proteins from TP3 to TP4 and TP6
343 (Supplemental Figure 1A). This shift in pN/pS may reflect the mixed signal of the two populations in TP4
344 and TP6 compared to the lower diversity populations in TP1 and TP3. The relative gene abundances
345 between populations mirror the allele frequency dynamics: we observed shifts in gene abundance between
346 TP1 and TP3, followed by gradual accumulation or loss of genes over time (Figure 3F; Supplemental
347 Data 5). Two sets of genes (NORP83 Gene IDs 2184-2186 and 2476-2477) were in TP1 at ~2× copies per

genome but dropped to <1× copies per genome for the other time points. These genes were annotated as part of a Type IV secretion system (IDs 2184-2186) and chromosome partitioning (ID 2477), which may indicate a role in horizontal gene transfer[45]. Conversely, two co-localized sets of genes were absent in TP1 (IDs 1472-1473, sugar permease; IDs 1719-1720, a putative sodium:proton antiporter and serine hydrolase) and had > 1× copies per genome in TP3 (Figure 3F; Supplemental Data 5). The sugar permease was absent in TP4 and TP6 (Figure 3F). Lastly of note, while present at <0.5× copies per genome in TP1, a set of genes (IDs 1027-1029) annotated as transposases increased in gene copy in TP3 (5-9× copies per genome) before dropping to an elevated level in TP4 and TP6 (2-6× copies per genome; Figure 3F; Supplemental Data 5). The accumulation of transposases may be indicative of genetic drift in this population[46], but based on the available data, it is challenging to distinguish between the forces of dispersal and drift in molding the population structure of NORP83. Regardless, the data indicate that the stochastic forces of drift and dispersal appear to have a stronger impact on population structure than selection in this crustal aquifer habitat.

The evidence suggests that the population represented by NORP163 (unknown *Gammaproteobacteria*) was also molded by a dispersal event. However, unlike NORP83 and NORP169, the variation in NORP163 appeared to be limited to a smaller section of the genome (Figure 3H). With sufficient coverage in five time points (TP0-TP2 and TP7-TP8) to accurately call SNVs, NORP163 was present in high abundance during the first five months of sampling, then persisted at lower abundance (0.24-3.43 RPKM) for seven months before increasing in abundance again (Figure 3G; Table 1). During the time points of interest, the nucleotide density remained relatively constant (20.0-32.1 SNVs kbp^{-1}). Despite the relatively consistent nucleotide density between TP0 and TP1, there was a sharp transition from the dominant alleles in TP0 to TP1 (Figure 3H). The alleles that shifted from TP0 to TP1 were not co-located in the genome, suggesting that rather than resulting from a gene-specific selective sweep, the shifts in allele frequency from TP0 to TP1 were introduced through dispersal (Supplemental Figure 2B). This interpretation is further supported by the fact that most of these alleles in TP2 are present at ~0.5 frequency, possibly resulting from the mixing of populations (Figure 3H). The population present in TP7-TP8 reflects the T1-population, but some alleles introduced in TP2 are still present. The SAAV/SNV ratio remained relatively constant across the time points of interest (Figure 3G), and there was no statistical change in pN/pS ratio in any of the KEGG categories (Supplemental Data 6). There were 45 putative genes that had shifts in frequency over the analyzed time points (Figure 3I; Supplemental Data 5). KEGG and GenBank annotations revealed that 12 of these genes were suspected transposases, with several exceeding >4× copies per genome in all of the time points (Figure 3I; Supplemental Data 5). There were at least five nonlocalized genes that were absent in TP0-TP2 and had >0× copies per genome in TP7-TP8 (NORP163 Gene IDs 167, 922, 1712, 1714, 2068; Figure 3I). These genes were annotated as ribosomal

382 proteins (167 and 2068), hypothetical proteins (IDs 922 and 1712), and a sulfite reductase (ID 1714;
383 Supplemental Data 5). A larger set of genes (some co-localized) changed from <1× copies per genome to
384 >1× copies per genome from TP0 to TP8 (Figure 3I; Supplemental Data 5). All of these genes were
385 ascribed annotations from GenBank with various functions, with only one annotated as a possible
386 transposase (Gene ID 465; Supplemental Data 5). The co-localized genes had functions related to core
387 carbon metabolism (Gene IDs 1083-1084), heavy metal sensing and transcriptional response (IDs 1589-
388 90), and osmolyte transport (IDs 1622-1623). While there was a trend towards increased gene copy
389 number over time for several of the genes identified in this MAG, we cannot state with certainty that
390 these genes provide a selective advantage for this variant.
391 For these MAGs (NORP83, NORP163, and NORP169) where allele frequency revealed the likely
392 mixing of at least two distinct populations, there were a few common threads. Dispersal not only had an
393 impact on which populations were present in the sample, but also the abundance of the population,
394 resulting in instances where the MAGs were virtually absent from the sample. While dispersal is a likely
395 mechanism driving the genome dynamics observed here, genetic drift cannot be discounted as a possible
396 evolutionary force. Both NORP83 and NORP163 had multiple transposases that shifted in copy number
397 over time. An increase in transposase activity has previously been identified as a signature for systems in
398 which drift may be the dominant evolutionary force, as it does not act to remove extrachromosomal
399 insertions from the population[46]. Further, many of the genes that had large changes in coverage confer
400 putative functions that could change the fitness of the population or provide specialization at the
401 intraspecific level, such that populations may compete for and/or maintain partially overlapping
402 ecological niches. In the instances where two (or more) populations mixed, as observed by allele
403 frequency, there generally was not a corresponding increase in abundance, perhaps reinforcing this idea
404 that the intraspecific populations shared an ecological niche rather than directly competed for it[44].
405
406 *Dispersal and evidence of selection.* While it appears that dispersal is a major factor influencing the
407 microbial population structure within the aquifer, there was evidence of gradual selection in NORP246
408 (*Shewenella*). NORP246 changed rapidly in abundance between TP0 (0.02 RPKM) and TP1 (11.60
409 RPKM), and thus would be a reasonable candidate for having undergone a clonal expansion in the three
410 months between samplings (Figure 4). However, in TP1, NORP246 had the highest initial nucleotide
411 diversity (46.7 SNVs kbp^{-1}) of all MAGs observed in their respective time points (Figure 1; Figure 4A).
412 This initial high nucleotide diversity in TP1 would be expected if the increase in abundance of the
413 NORP246 population resulted from the migration of an extant population into the borehole. For the three
414 time points of interest (TP1, TP3, and TP4), there was a corresponding gradual decrease in abundance
415 (11.60 to 5.24 RPKM), which may be indicative of cell death (Figure 4A). This gradual decline was

interrupted by a sharp drop in abundance in TP2 (0.02 RPKM; equivalent to approximately 3 cells mL^{-1}). When the population rebounded in TP3 (8.34 RPKM) there was no evidence of clonal expansion, as nucleotide diversity remained high (29.11 SNVs kbp^{-1}), which is likely indicative of a dispersal event that transported most NORP246 cells out of the borehole in TP2 before returning in TP3. As abundance decreased, so did nucleotide diversity. The allele frequency reveals a transition from fairly even allele representation in TP1 towards fixation for many sites in TP4 (Figure 4B). A statistically significant drop in pN/pS from TP1 to TP3 and TP4 for the "No KEGG annotation" category may reveal an increase in purifying selection (Supplemental Figure 1). Collectively, the gradual shift in allele frequency combined with a decrease in pN/pS may be indicative of an increase in purifying selection operating on the NORP246 population (Figure 4).

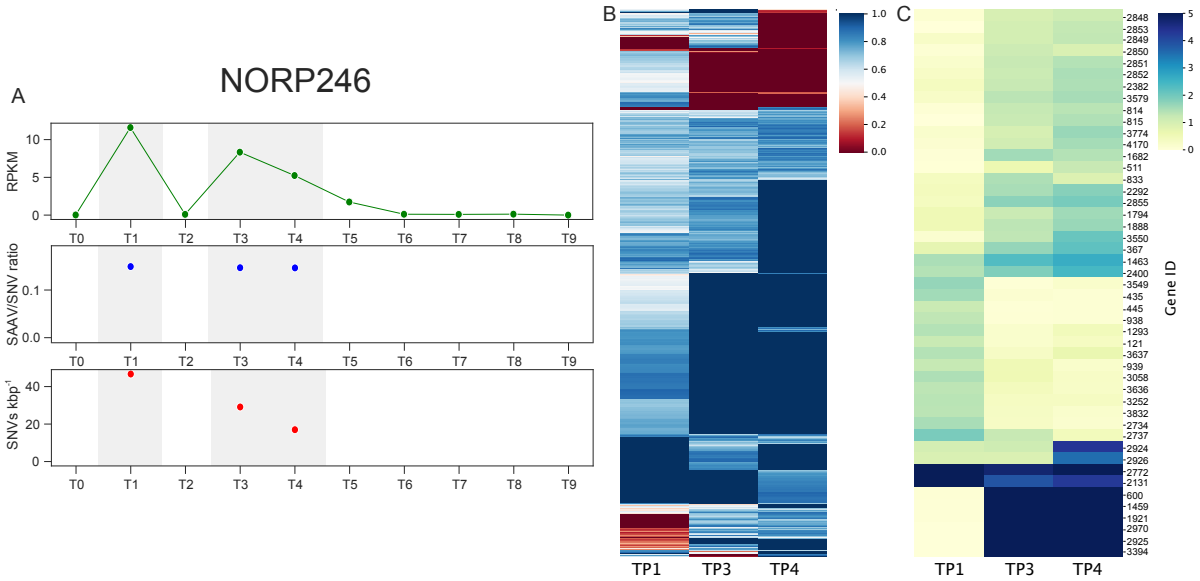

Figure 4. Intraspecific population metrics for NORP246. **A.** Scatterplots tracking RPKM, SAAV/SNV ratio, and SNVs kbp^{-1} across the time-series. Grey boxes highlight the time points of interest (≥ 5 RPKM). SAAV/SNV ratio and SNVs kbp^{-1} in low abundance time points have been removed. **B.** Hierarchically clustered heatmap of allele frequency and identified SNV location. Scaled from 0-1. Both 0.0 and 1.0 represent a fixed allele; 0.5 represents a split allele. **C.** Hierarchically clustered heatmap of gene frequencies for genes ≥ 1× change in coverage over the time points of interest. Scaled range from 0-5× copies. Maximum value of gene frequency in C is 21.7× copies. Supplemental Data 5.

Changes in gene copy number accompanied the shift in allele frequencies. Forty-seven putative genes changed substantially in frequency over three time points in the NORP246 population (Figure 4C). These genes can be divided into three broad groups: (1) present in TP1 and absent in TP3 and TP4, (2) absent in TP1 and present in TP3 and TP4, and (3) absent in TP1 and present in high coverage in TP3 and TP4. The 13 putative genes in group 1 were present in TP1 (~1× copies per genome) and absent in TP3 and TP4 predominantly annotated as hypothetical proteins with some conserved domains (n = 7; Figure 4C). Three of the putative genes had roles in transport: xanthine permease (ID 1682), sodium/glutamate symporter (ID 833), and cobalt ATP binding cassette-type permease (ID 2292; Supplemental Data 6). Two co-localized genes in this group were annotated as a transposase and reverse transcriptase (IDs 3549-

435 3550; Supplemental Data 6). Conversely, the 23 putative genes in group 2 were absent in TP1 (<1×
436 copies per genome) and present in TP3 and TP4 (1-2× copies per genome) and were predominantly
437 annotated as hypothetical proteins with conserved domains (n = 18; Figure 4C). The other five putative
438 genes in group 2 were not co-localized and had nonspecific functional annotations except for a fumarate
439 reductase subunit C (ID 3394; Supplemental Data 6). Genes in group 3, which were absent in TP1 and
440 present in high coverage in TP3 and TP4 (15-20× copies per genome), were co-localized (IDs 2848-2853)
441 and lack annotations, except for gene ID 2851 with homology to proteins in GenBank annotated as DNA
442 replication protein (Figure 4C; Supplemental Data 6). This segment appeared to contain a fragment of
443 DNA that in TP3 and TP4 was independently replicating relative to the NORP246 genome, possibly a
444 plasmid or similar extrachromosomal element. The lack of annotations makes it impossible to determine
445 the roles of these genes within the TP3- and TP4- populations, but the loss of several transporters from
446 the TP1-population and the observed increase in purifying selection may reflect selection pressure
447 towards a shift in cellular priorities for NORP246.
448
449 *Relaxed purifying selection.* Amongst all of the MAGs analyzed here, NORP139 (unknown
450 *Parvibaculaceae*) had unique patterns of genomic variation (Figure 5). Unlike all of the other MAGs,
451 NORP139 was present in relatively high abundance at all time points in the time-series. This MAG had
452 sufficient coverage to accurately call SNVs in five time points (TP1, TP2 and TP4-TP6) and was
453 consistently present in other time points at lower abundance values, except in TP9 (1.21-4.37 RPKM;
454 Table 1; Figure 5A). Moreover, the NORP139 population accumulated SNVs over time. The shift from
455 fixed alleles in TP1, TP2, and TP4 to an increased number of variable sites in TP5 and TP6 may be
456 indicative of changes in selection pressure (Figure 5B). This variation coincides with changes in observed
457 pN/pS values in two functional categories (Supplemental Figure 1B & C). While the increase in
458 nucleotide diversity did not translate to changes in the SAAV/SNV ratio, there was a statistically
459 significant increase in pN/pS for both the "No KEGG annotation" and Energy Metabolism category
460 (KEGG Category 09102) between several time points (Supplemental Figure 1B & C). This change in
461 pN/pS suggested a shift toward diversifying selection or more relaxed purifying selection between time
462 points, specifically between TP4, TP5, and TP6. The Energy Metabolism genes with a pN/pS shift
463 consisted of 25 putative genes that have annotations as part of carbon, nitrogen, sulfur transformations
464 (Supplemental Data 6). However, most of the annotations (n = 16) were for genes that are part of the
465 oxidative phosphorylation process, specifically, components of complexes I (NADH dehydrogenase;
466 NuoCDEFGHIJKLM), II (succinate dehydrogenase; SdhCDB), and IV (cytochrome c oxidase; CoxCA)
467 of the electron transport chain. Unlike other persisters, NORP139 had very few genes (n = 5) with
468 differences in gene frequency (Figure 5C). Four of the five were hypothetical in nature and the remaining

469 gene was annotated as the large subunit ribosomal protein L32, which fluctuates from 1× to 2× copies per
470 genome in TP2 (Figure 5C; Supplemental Data 6). The gradual increase in diversity within the NORP139
471 population suggested a limited influence of either natural selection or genetic drift in removing variation
472 from the population during the study period. Although there was an observed shift in the selection
473 pressure for some genes, especially related to the electron transport chain, selection was weak and did not
474 result in a broad population sweep.

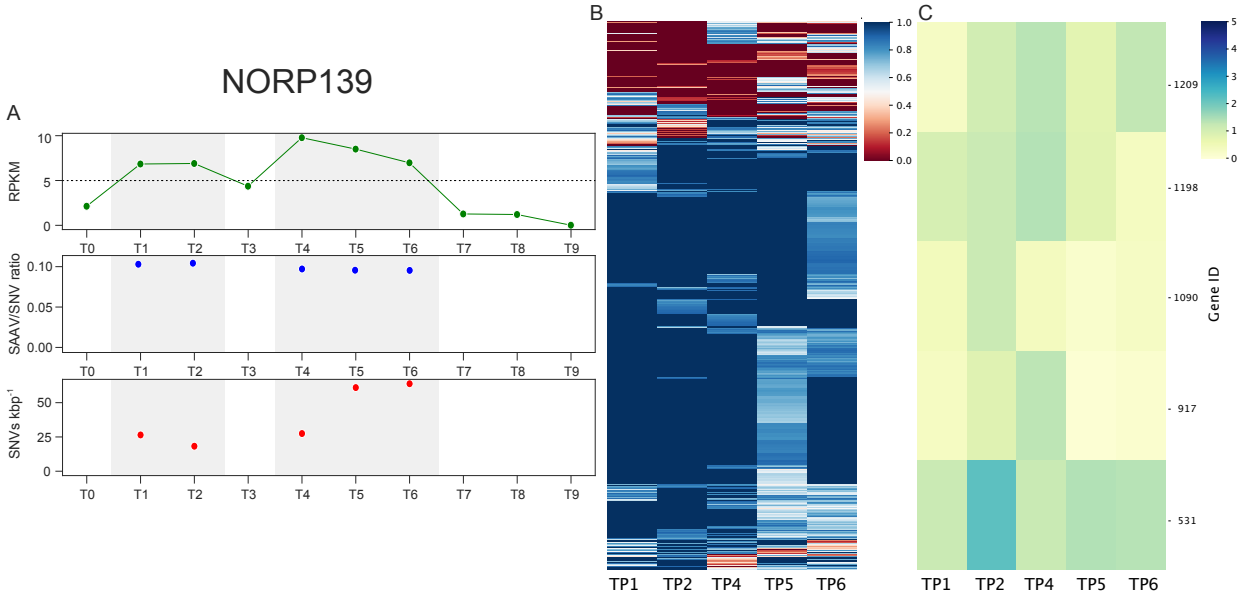

Figure 5. Intraspecific population metrics for NORP139. **A.** Scatterplots tracking RPKM, SAAV/SNV ratio, and SNVs kbp^{-1} across the time-series. Grey boxes highlight the time points of interest (≥ 5 RPKM). SAAV/SNV ratio and SNVs kbp^{-1} in low abundance time points have been removed. **B.** Hierarchically clustered heatmap of allele frequency and identified SNV location. Scaled from 0-1. Both 0.0 and 1.0 represent a fixed allele; 0.5 represents a split allele. **C.** Hierarchically clustered heatmap of gene frequencies for genes ≥ 1× change in coverage over the time points of interest. Range from 0-5× copies.

475 **Conclusions**

476 The MAGs described here represent subseafloor microbial populations that exhibited substantial changes
477 in size over the ~825-day sampling period. Thus, these datasets provide evidence that the marine crustal
478 aquifer represents a dynamic habitat in which microbial populations grow and decay and can be dispersed
479 over monthly timescales. The rapid shifts in allele frequencies and nucleotide diversity suggest that
480 stochastic events, such as genetic drift associated with population bottlenecks or dispersal and mixing of
481 populations through the aquifer, play an important role in molding the evolutionary trajectories of
482 microbial populations in this habitat[47]. Though classically structured as the introduction of mutation or
483 removal of mutations through selection and drift, evolution, broadly defined, reflects changes in allele
484 frequency within a population. Thus, dispersal can introduce extant populations from elsewhere in the
485 environment and the interaction of these newly introduced alleles with the environment reflects an
486 evolutionary response. As such, we are able to observe microbial evolution in action in the fluids moving
487 through the oceanic crust. The observed population shifts occur in the span of months, reflecting the

488 highly dynamic nature of the system, both biologically and physically. While rapid allele frequency shifts
489 can be linked to different types of population interactions, such as sweeps, dispersal, and clonal
490 expansion, dispersal appears to play an important role in structuring the most abundant populations in the
491 crustal fluid samples. As noted above, it is difficult to distinguish the relative contributions of dispersal
492 (*i.e.*, changing allele frequencies due to physical movement of populations) and genetic drift (*i.e.*,
493 changing allele frequencies due to stochastic events) in driving changing allele frequencies in these
494 habitats. The accumulation of extrachromosomal insertions, such as transposable elements and plasmid
495 insertions, suggests that drift can impact these populations in a manner distinct from dispersal. In
496 summary, the subseafloor aquifer of North Pond represents a highly dynamic habitat where evolution may
497 be governed largely by the stochastic forces of dispersal and drift.
498
499 **Data Availability**
500 Elements for this project can be found deposited at DDBJ/ENA/GenBank under the BioProject accession
501 no. PRJNA391950. Raw sequence reads are available through the Short Read Archive with the accession
502 no. SRX3143886-SRX3143902. Raw sequence reads from Meyer *et al*. (20) constituting the
503 metagenomic samples from 2012, are available under the BioProject accession no. PRJNA280201.
504 Additional files, including the contigs, anvi'o protein calls, and anvi'o database profiles for the MAGs
505 used in this analysis, are available through figshare (doi: 10.6084/m9.figshare.13568549). As detailed in
506 Supplemental Data 1, all new/updated MAGs have been submitted to NCBI under the BioProject
507 accession no. PRJNA391950.
508
509 **Acknowledgements**
510 We thank the crews of the *R/V* Merian and *ROV* Jason II, Wolfgang Bach, Peter Girguis, Chih-Chiang
511 Hsieh, Ulrike Jaekel, Beate Kraft, Huei-Ting Lin, Beth Orcutt, Keir Becker, Stephanie Carr, and Heiner
512 Villinger for support in accomplishing the 2012 and 2014 field programs. Ship time was provided by the
513 German Science Foundation (DFG). Both Katrina Edwards and James Cowen's efforts were critical to the
514 field component and success of this project. They are missed immensely. Leslie Murphy and Emily
515 Reddington provided laboratory support at the WM Keck sequencing facility at the Marine Biological
516 Laboratory. This work was supported by NSF OCE-1062006, OCE-1745589 and OCE-1635208 to J.A.H.
517 The Gordon and Betty Moore Foundation sponsored observatory components at North Pond through
518 grant GBMF1609. The Center for Dark Energy Biosphere Investigations (C-DEBI) (OCE-0939564)
519 supported J.A.H. and B.J.T. This is C-DEBI contribution XXX.
520
521 **Author Contributions**

522 Analyses were conducted by R.E.A., E.D.G., and B.J.T. E.D.G. performed the multi-tiered binning
523 approach that generated the new MAGs. R.E.A. and B.J.T. performed the population analysis. R.E.A. and
524 B.J.T. wrote the manuscript. All authors reviewed and edited the manuscript. J.A.H. was the lead
525 researcher on establishing North Pond as a long-term research site and supported the collection and
526 processing of all samples. The study was conceived by R.E.A. and B.J.T.
527
528 The authors declare no conflict of interest.
529
530 **Figure Legends**
531 Figure 1. Scatter plot of the nucleotide diversity for each of the six "persister" and four "bloomer" MAGs
532 for the ten time points sampled from North Pond CORK U1382A. The size of each point is scaled by the
533 RPKM in the time point. Only time points with ≥ 5 RPKM are included. Lines denote points from the
534 same MAG and do not display continuous data.
535 Figure 2. Intraspecific population metrics for NORP147. **A.** Scatterplots tracking RPKM, SAAV/SNV
536 ratio, and SNVs kbp^{-1} across the time-series. Grey boxes highlight the time points of interest (≥ 5 RPKM).
537 SAAV/SNV ratio and SNVs kbp^{-1} in low abundance time points have been removed. **B.** Hierarchically
538 clustered heatmap of allele frequency at each identified SNV location. Scaled from 0-1. Both 0.0 and 1.0
539 represent a fixed allele; 0.5 represents a split allele.
540 Figure 3. Intraspecific population metrics for NORP83, NORP163, and NORP169. **A, D, G.** Scatterplots
541 tracking RPKM, SAAV/SNV ratio, and SNVs kbp^{-1} across the time-series. Grey boxes highlight the time
542 points of interest (≥5 RPKM). SAAV/SNV ratio and SNVs kbp^{-1} in low abundance time points have been
543 removed. The y-axes across MAGs are not held constant. **B, E, H.** Hierarchically clustered heatmap of
544 allele frequency and identified SNV location. Scaled from 0-1. Both 0.0 and 1.0 represent a fixed allele;
545 0.5 represents a split allele. **C, F, I.** Hierarchically clustered heatmap of gene frequencies for genes ≥ 1×
546 change in coverage over the time points of interest. Scaled range from 0-5× copies. Maximum value of
547 gene frequency in F and G is 9.5× and 6.5× copies, respectively. Supplemental Data 5.
548 Figure 4. Intraspecific population metrics for NORP246. **A.** Scatterplots tracking RPKM, SAAV/SNV
549 ratio, and SNVs kbp^{-1} across the time-series. Grey boxes highlight the time points of interest (≥ 5 RPKM).
550 SAAV/SNV ratio and SNVs kbp^{-1} in low abundance time points have been removed. **B.** Hierarchically
551 clustered heatmap of allele frequency and identified SNV location. Scaled from 0-1. Both 0.0 and 1.0
552 represent a fixed allele; 0.5 represents a split allele. **C.** Hierarchically clustered heatmap of gene
553 frequencies for genes ≥ 1× change in coverage over the time points of interest. Scaled range from 0-5×
554 copies. Maximum value of gene frequency in C is 21.7× copies. Supplemental Data 5.

Figure 5. Intraspecific population metrics for NORP139. **A.** Scatterplots tracking RPKM, SAAV/SNV ratio, and SNVs kbp^{-1} across the time-series. Grey boxes highlight the time points of interest (≥ 5 RPKM). SAAV/SNV ratio and SNVs kbp^{-1} in low abundance time points have been removed. **B.** Hierarchically clustered heatmap of allele frequency and identified SNV location. Scaled from 0-1. Both 0.0 and 1.0 represent a fixed allele; 0.5 represents a split allele. **C.** Hierarchically clustered heatmap of gene frequencies for genes ≥ 1× change in coverage over the time points of interest. Range from 0-5× copies.

References

1. Kallmeyer, J., Pockalny, R., Adhikari, R. R., Smith, D. C. & D'Hondt, S. Global distribution of microbial abundance and biomass in subseafloor sediment. *Proceedings of the National Academy of Sciences* **109,** 16213–16216 (2012).
2. Parkes, R. J. *et al.* A review of prokaryotic populations and processes in sub-seafloor sediments, including biosphere:geosphere interactions. *Marine Geology* **352,** 409–425 (2014).
3. Bradley, J. A. *et al.* Widespread energy limitation to life in global subseafloor sediments. *Sci Adv* **6,** eaba0697 (2020).
4. Inagaki, F. *et al.* Exploring deep microbial life in coal-bearing sediment down to ~2.5 km below the ocean floor. *Science* **349,** 420–424 (2015).
5. D'Hondt, S. *et al.* Presence of oxygen and aerobic communities from sea floor to basement in deep-sea sediments. *Nature Geoscience* **8,** 299–304 (2015).
6. Tully, B. J., Wheat, C. G., Glazer, B. T. & Huber, J. A. A dynamic microbial community with high functional redundancy inhabits the cold, oxic subseafloor aquifer. *ISME J* **12,** 1–16 (2018).
7. Kashtan, N. *et al.* Single-cell genomics reveals hundreds of coexisting subpopulations in wild Prochlorococcus. *Science* **344,** 416–420 (2014).
8. Denef, V. J. & Banfield, J. F. In situ evolutionary rate measurements show ecological success of recently emerged bacterial hybrids. *Science* **336,** 462–466 (2012).
9. Bendall, M. L. *et al.* Genome-wide selective sweeps and gene-specific sweeps in natural bacterial populations. *ISME J* (2016). doi:10.1038/ismej.2015.241
10. Anderson, R. E. *et al.* Genomic variation in microbial populations inhabiting the marine subseafloor at deep-sea hydrothermal vents. *Nature Communications* 1–11 (2017). doi:10.1038/s41467-017-01228-6
11. Edwards, K. J., Bach, W. & Klaus, A. Mid-Atlantic Ridge flank microbiology: initiation of long-term coupled microbiological, geochemical, and hydrological experimentation within the seafloor at North Pond, western flank of the Mid-Atlantic Ridge. *IODP Sci Prosp 336* 1–62 (2010). doi:10.2204/ iodp.sp.336.2010
12. Sclater, J. G., Jaupart, C. & Galson, D. The heat flow through oceanic and continental crust and the heat loss of the Earth. *Reviews of Geophysics* **18,** 269–311 (1980).
13. Stein, C. A. & Stein, S. Constraints on hydrothermal heat flux through the oceanic lithosphere from global heat flow. *Journal of Geophysical Research: Solid Earth* **99,** 3081–3095 (1994).
14. Johnson, H. P. & Pruis, M. J. Fluxes of fluid and heat from the oceanic crustal reservoir. *Earth and Planetary Science Letters* **216,** 565–574 (2003).
15. Davis, E. E., Becker, K., Pettigrew, T., Carson, B. & MacDonald, R. CORK: a hydrologic seal and downhole observatory for deep-ocean boreholes. *Proceedings of the Ocean Drilling Program, Initial Reports* **139,** 43–53 (1992).
16. Wheat, C. G. *et al. Fluid sampling from oceanic borehole observatories: design and methods for CORK activities (1990-2010)*. 1–36 (Integrated Ocean Drilling Program, 2011). doi:10.2204/iodp.proc.327.109.2011

17. Seyler, L. M., Trembath-Reichert, E., Tully, B. J. & Huber, J. A. Time-series transcriptomics from cold, oxic subseafloor crustal fluids reveals a motile, mixotrophic microbial community. *ISME J* **18,** 1–15 (2020).
18. Walter, S. R. S. *et al.* Microbial decomposition of marine dissolved organic matter in cool oceanic crust. *Nature Geoscience* **11,** 1–8 (2018).
19. Wheat, C. G. *et al.* Subseafloor Cross-Hole Tracer Experiment Reveals Hydrologic Properties, Heterogeneities, and Reactions in Slow-Spreading Oceanic Crust. *Geochem. Geophys. Geosyst.* **21,** 2900–15 (2020).
20. Meyer, J. L. *et al.* A distinct and active bacterial community in cold oxygenated fluids circulating beneath the western flank of the Mid-Atlantic ridge. *Sci. Rep.* **6,** 22541 (2016).
21. Starnawski, P. *et al.* Microbial community assembly and evolution in subseafloor sediment. *Proc. Natl. Acad. Sci. U.S.A.* **114,** 2940–2945 (2017).
22. Price, A. N., Fisher, A. T., Weathers, T. S., Gable, C. W. & Stauffer, P. H. Two- and Three-Dimensional Numerical Simulations of Coupled Fluid and Heat Flow Processes Beneath a Marine Sediment Pond. *AGU Fall Meeting Abstracts* **2019,** V33E–0237 (2019).
23. Cowen, J. P. *et al.* Advanced instrument system for real-time and time-series microbial geochemical sampling of the deep (basaltic) crustal biosphere. *Deep-Sea Research Part I* **61,** 43–56 (2012).
24. Lin, H.-T., Hsieh, C.-C., Repeta, D. J. & Rappé, M. S. Sampling of basement fluids via Circulation Obviation Retrofit Kits (CORKs) for dissolved gases, fluid fixation at the seafloor, and the characterization of organic carbon. *MethodsX* **7,** 101033 (2020).
25. Sogin, M. L. *et al.* Microbial diversity in the deep sea and the underexplored 'rare biosphere'. *Proceedings of the National Academy of Sciences* **103,** 12115–12120 (2006).
26. Martin, M. Cutadapt removes adapter sequences from high-throughput sequencing reads. *EMBnet.journal* **17,** (2011).
27. Bolger, A. M., Lohse, M. & Usadel, B. Trimmomatic: a flexible trimmer for Illumina sequence data. *Bioinformatics* **30,** 2114–2120 (2014).
28. Eren, A. M. *et al.* Anvi'o: an advanced analysis and visualization platform for 'omics data. *PeerJ* **3,** e1319 (2015).
29. Langmead, B. & Salzberg, S. L. Fast gapped-read alignment with Bowtie 2. *Nat Meth* **9,** 357–359 (2012).
30. Li, H., Handsaker, B., Fennell, T., Ruan, J. & Homer, N. The Sequence Alignment/Map format and SAMtools. *Bioinformatics* **25,** 2078–2079 (2009).
31. Liao, Y., Smyth, G. K. & Shi, W. featureCounts: an efficient general purpose program for assigning sequence reads to genomic features. *Bioinformatics* **30,** 923–930 (2014).
32. Graham, E. D., Graham, E. D., Heidelberg, J. F. & Tully, B. J. BinSanity: unsupervised clustering of environmental microbial assemblies using coverage and affinity propagation. *PeerJ* **5,** e3035–19 (2017).
33. McLaren, M. R., Willis, A. D. & Callahan, B. J. Consistent and correctable bias in metagenomic sequencing experiments. *eLife* **8,** 365 (2019).
34. Bendall, M. L. *et al.* Genome-wide selective sweeps and gene-specific sweeps in natural bacterial populations. **10,** 1589–1601 (2016).
35. Jain, C., Rodriguez-R, L. M., Phillippy, A. M., Konstantinidis, K. T. & Aluru, S. High throughput ANI analysis of 90K prokaryotic genomes reveals clear species boundaries. *Nature Communications* **9,** 7200–8 (2018).
36. Rodriguez-R, L. M., Tsementzi, D., Luo, C. & Konstantinidis, K. T. Iterative subtractive binning of freshwater chronoseries metagenomes identifies over 400 novel species and their ecologic preferences. *Environ. Microbiol.* **22,** 3394–3412 (2020).
37. Kanehisa, M., Sato, Y. & Morishima, K. BlastKOALA and GhostKOALA: KEGG Tools for Functional Characterization of Genome and Metagenome Sequences. *Journal of Molecular Biology* **428,** 726–731 (2016).

652 38. Chaumeil, P.-A., Mussig, A. J., Hugenholtz, P. & Parks, D. H. GTDB-Tk: a toolkit to classify
653 genomes with the Genome Taxonomy Database. *Bioinformatics* 1–3 (2019).
654 doi:10.1093/bioinformatics/btz848
655 39. Mann, H. B. & Whitney, D. R. On a test of whether one of two random variables is stochastically
656 larger than the other. *Annals of Mathematical Statistics* **18,** 50–60 (1947).
657 40. Benjamini, Y. & Hochberg, Y. Controlling the False Discovery Rate: A Practical and Powerful
658 Approach to Multiple Testing. *Journal of the Royal Statistical Society. Series B Methodological*
659 **57,** 289–300 (1995).
660 41. Van Rossum, T., Ferretti, P., Maistrenko, O. M. & Bork, P. Diversity within species: interpreting
661 strains in microbiomes. *Nature* **37,** 463–16 (2020).
662 42. Shapiro, B. J. & Polz, M. F. Ordering microbial diversity into ecologically and genetically
663 cohesive units. *Trends in Microbiology* **22,** 235–247 (2014).
664 43. Garud, N. R., Good, B. H., Hallatschek, O. & Pollard, K. S. Evolutionary dynamics of bacteria in
665 the gut microbiome within and across hosts. *Plos Biol* **17,** e3000102–29 (2019).
666 44. Garcia, S. L. *et al.* Contrasting patterns of genome-level diversity across distinct co-occurring
667 bacterial populations. *ISME J* **12,** 1–14 (2018).
668 45. Wallden, K., Rivera-Calzada, A. & Waksman, G. Microreview: Type IV secretion systems:
669 versatility and diversity in function. *Cellular Microbiology* **12,** 1203–1212 (2010).
670 46. Escobar-Páramo, P., Ghosh, S. & DiRuggiero, J. Evidence for Genetic Drift in the Diversification
671 of a Geographically Isolated Population of the Hyperthermophilic Archaeon Pyrococcus.
672 *Molecular Biology and Evolution* **22,** 2297–2303 (2005).
673 47. Schloissnig, S. *et al.* Genomic variation landscape of the human gut microbiome. *Nature* **493,** 1–6
674 (2012).